Picosecond photofragment spectroscopy. III. Vibrational predissociation of van der Waals' clusters

Joseph L. Knee, Lutfur R. Khundkar, and Ahmed H. Zewail

Citation: The Journal of Chemical Physics **87**, 115 (1987); doi: 10.1063/1.453608
View online: http://dx.doi.org/10.1063/1.453608
View Table of Contents: http://scitation.aip.org/content/aip/journal/jcp/87/1?ver=pdfcov
Published by the AIP Publishing

Picosecond photofragment spectroscopy. III. Vibrational predissociation of van der Waals' clusters

Joseph L. Knee,[a] Lutfur R. Khundkar, and Ahmed H. Zewail
Arthur Amos Noyes Laboratory of Chemical Physics,[b] California Institute of Technology, Pasadena, California 91125

(Received 9 December 1986; accepted 11 February 1987)

This paper, last in this series, reports on the picosecond dynamics of vibrational predissociation in beam-cooled van der Waals' clusters. Reaction rates have been measured for clusters (1:1) of phenol and cresol (*p*-methylphenol) with benzene by the picosecond pump–probe photoionization mass-spectrometry technique. Dissociation to form phenol (cresol) and benzene takes place from vibrational levels of the S_1 state of phenol (cresol) prepared by the pump laser. The predissociation rates were measured for a number of different excess energies upto $\sim 2500\ cm^{-1}$, and the reaction threshold was found to be $1400\ cm^{-1}$ above the S_1 origin for phenol–benzene and $\sim 1795\ cm^{-1}$ for cresol–benzene, respectively. For phenol–benzene, the predissociation rates, following excitation of ring-type modes, vs excess energy vary more or less smoothly. Cresol–benzene exhibits biexponential decay, with the fast component becoming more dominant at higher energies. A non-RRKM model involving division of the vibrational phase space is discussed to explain this observation.

I. INTRODUCTION

van der Waals molecules have been the focus of intense study since the development of supersonic molecular beams and sensitive spectroscopic tools for measuring their properties.[1] The interest stems from the fact that these are simple systems dominated by long range attractive forces which are manifested as small perturbations of the constituent molecules. Studying such systems may allow one to understand interactions which are important to energy flow in dissociating complex systems and to the structure of more strongly bound chemical species. Much of the work to date has focused on the spectroscopy of these species as a means of determining the structure, interaction potentials, stabilization energies and induced perturbations present which all help to describe the bonding in these model systems.

Our primary interest in van der Waals molecules is their use as model systems for studying chemical reactivity, specifically IVR dynamics and unimolecular dissociation. The presence of a van der Waals bond between two constituent molecules induces only a small perturbation allowing the system to be approximated by the states of the uncomplexed molecules. The important feature for unimolecular dissociation of such species is that the van der Waals bond is much weaker than any of the covalent bonds in the system and therefore only a moderate amount of energy need be deposited in one of the constituent molecules to exceed the van der Waals dissociation energy. This amount of energy places the chromophore on an excited part of its potential energy surface which is still adequately described by the normal vibrational modes of the system. In other words, the small amount of energy to break the van der Waals bond can be deposited in the system by exciting a well defined initial state whereas to break a chemical bond in a strongly bound species, the system has to be excited to a portion of the potential energy surface where anharmonic and Coriolis couplings are important. Thus van der Waals molecules should be simple model systems to test theoretical descriptions because one can be more concerned with the influence of the few intermolecular modes than with describing a highly excited region of a multidimensional potential surface. They also provide a testing ground for the fundamental problem of energy flow to the reaction coordinate. If energy redistribution is complete prior to vibrational predissociation, one should observe dynamical behavior predicted by statistical theories. On the other hand, if dissociation rates are comparable to the rate of redistribution, then mode specific (selective) effects may be present.

Until now almost all of the information on van der Waals molecule predissociation has come from spectroscopic measurements which fall into two categories. The first is the measurement of electronic state spectra where predissociation occurs on an excited state potential. Here, the presence of predissociation is observed as either a broadening in the absorption spectrum (either fluorescence excitation or MPI spectra) or a change in the fluorescence from the excited state due to vibrational (but not electronic) relaxation of the initially prepared excited state caused by the predissociation process. A prototype study of this kind is that of I_2–He,[2] and a large number of systems have now been studied.[3] The information one can obtain includes the van der Waals binding energy (by observation of the predissociation threshold) and possibly the product states of the dissociation, observed by monitoring the fluorescence spectrum of the initially excited molecule which has now been vibrationally relaxed. The second type of experiment is direct excitation to vibrational states in the ground electronic state of one of the constituent molecules. Although these experiments are more attractive because one does not have to be concerned with influences of excited electronic states, they are technically more difficult. A number of such experiments have been done with available lasers,[4] often line tunable ones such as

[a] Present address: Dept. of Chemistry, Wesleyan University, Middletown, CT 06547.
[b] Contribution No. 7515.

 0021-9606/87/130115-13$02.10

CO_2, and they have been mostly concerned with measuring linewidths to determine the spectral broadening due to the presence of relatively fast predissociation processes. One advantage of this approach is that small molecules can be studied which is often not the case with the electronic state spectroscopy approach because the smaller molecules (unlike I_2) generally do not absorb in wavelength regions conveniently accessed by present day lasers (>200 nm). From doing either type of spectroscopy one can learn about the energetics of the predissociation process such as the reaction barrier height and product state distributions. One could also obtain the rates for the predissociation process if the relationship between linewidths and rates is well defined.

In general, linewidths and lifetimes are not related unless one knows with certainty that the line is homogeneously broadened and that no dephasing is involved.[5] In diatomics, the relationship is clear and has been confirmed experimentally.[6] In larger systems, contributions to the measured linewidths from inhomogeneous broadening, power saturation effects, and pure dephasing are difficult to ascertain, and care must be exercised in relating linewidths to dynamics.[7]

Several reports have appeared where time resolved fluorescence has been used to measure vdW molecule dissociation rates by monitoring fluorescence decay rates. Spectral and time resolution of the fluorescence on the picosecond time scale[8] allows one to obtain the rates of intramolecular vibrational redistribution (IVR) and vibrational predissociation (VP). When one measures the VP process directly in time the actual rate, and not the dephasing time of the initially prepared state, is obtained. The van der Waals systems studied by this technique are isoquinoline–water,[9] tetrazine–Ar,[10] dimethyl tetrazine dimer,[11] stilbene–He and –Ar,[12] and anthracene–Ar.[12] In these studies the stoichiometry of the complex is inferred spectroscopically. Only very recently, a high-resolution sub-Doppler method has been used to measure the stoichiometry of these large complexes.[12] The time resolution of these fluorescence experiments is $\sim$100–40 ps.

In a recent communication,[13] we reported our results on the direct measurement of van der Waals molecule VP rates using picosecond pump–probe mass spectrometry. This technique uses two picosecond pulses, one to excite the vdW complex and the second, delayed in time, to ionize the excited complexes. The ions are identified by their mass in a time-of-flight spectrometer. The time resolution is a few picoseconds in this case, limited by the temporal width of the laser pulses. The system studied was phenol–benzene.

In this paper we give a full account of the study of the phenol–benzene complex (Ph–Bz) and extend it to the cresol–benzene (*p*-methylphenol–benzene) system; the binding energy of the complexes (Fig. 1) is $\sim$4 kcal/mol. Substituting phenol with a methyl group allows us to control the density of states in the system without making substantial changes in the electronic structure. The results can then be compared in a relative sense which is particularly important for RRKM calculations. Furthermore, in both systems the excitation is to phenol type modes and this permits the study of energy redistribution from the phenol moiety to the reaction coordinate. The questions pertinent to the dynamics

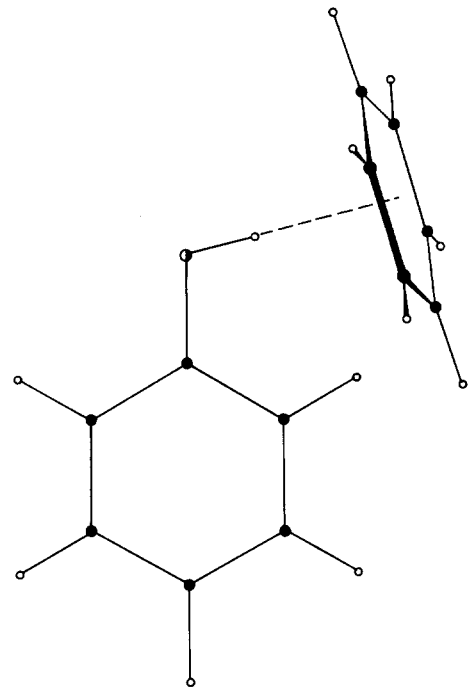

FIG. 1. Representation of the phenol–benzene van der Waals binding geometry. The interaction is π electron hydrogen bonding with the phenol "donating" a proton to the π cloud of benzene. This structure is supported by both thermodynamic and spectroscopic data and should be almost identical in the *p*-cresol–benzene system. The binding energy is estimated to be 1400 cm^{-1} (see the text).

are: (1) What is the extent of intramolecular vibrational redistribution prior to dissociation? (2) Are the dissociation rates dependent only on excess energy or are they mode specific? (3) Can the rates in these simple systems be predicted by statistical reaction rate theories?

The paper is outlined as follows. The experimental scheme is described in detail first (Sec. II). A brief survey of the decays (Sec. III A) is followed by excitation spectra of cresol and its complex with benzene (Sec. III B). Discussion of our interpretation of the observed transient behavior is presented next (Sec. III C), followed by discussion of the VP rates for each of the two systems in the last four subsections.

II. EXPERIMENTAL

A. General

The aim of the experiments is to measure the unimolecular dissociation rates of the Ph–Bz system when vibrational energy is deposited initially in the phenol moiety. The excitation of phenol is an electronic transition which allows a variety of vibrational states in the S_1 manifold to be accessed from which predissociation occurs on the excited electronic surface. To measure the unimolecular dissociation rates we use a picosecond pump–probe photoionization technique which is described as follows (Fig. 2). The Ph–Bz species is excited via the phenol $S_0 \rightarrow S_1$ transition with a UV picosecond laser pulse. A second, red-shifted, picosecond pulse then excites this species above its ionization threshold. The resulting product ions are mass analysed in a time of flight

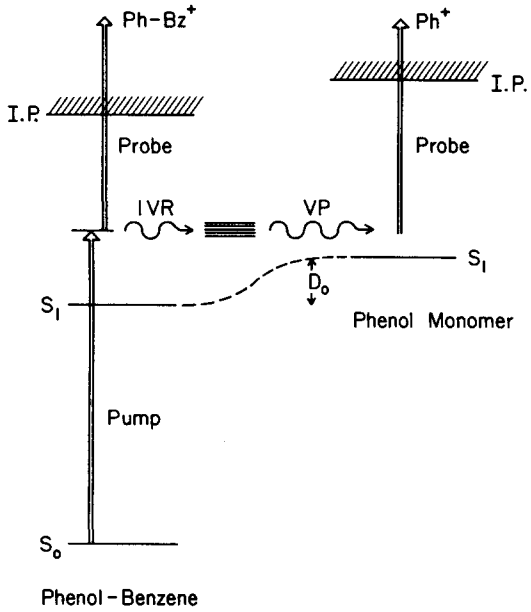

FIG. 2. Schematic energy level diagram of the phenol–benzene system showing the correlation from the bound system to free phenol along the reaction coordinate. The pump and probe scheme is shown. The case described here is that of IVR followed by VP. The second channel, not shown, is that of the initial state undergoing direct VP to products.

mass spectrometer. By monitoring the amount of parent ion formed ($[Ph–Bz]^+$) as a function of pump–probe pulse delay we can measure directly the vibrational predissociation rates because any dissociation which takes place in the neutral, between the pump and probe pulses, will be observed as a loss of signal in the parent ion mass channel. A discussion of possible alternative processes which may lead to similar observations will be presented below but they can be ruled out, leaving the observation of decay of the parent ion signal as being a measure of vibrational predissociation of the complex from the S_1 state of phenol. The dissociation rates can then be measured as a function of excess energy and vibrational state character by pumping a variety of vibrational states in phenol. The same experiments were also performed on cresol–benzene van der Waals molecules.

B. Laser system: Pump and probe

The pump–probe laser arrangement is described in the preceding papers I and II.[14] The picosecond system used in this work is different from that given in papers I and II. In the previous papers we used two separate dye-laser/amplifier units, starting with a mode-locked cw YAG laser. Here, a mode-locked Ar^+ laser and one dye-laser/amplifier system was used. The experimental apparatus with MPI detection has been described only briefly in several publications[15] so a more detailed description will be given here. To perform the ionization experiments outlined above, high peak power picosecond laser pulses are required with the necessity also of having pump and probe pulses in the UV but different wavelengths for greater sensitivity. This is accomplished using a pulse amplified picosecond laser system. The picosecond pulses originate in a mode locked argon ion laser which is synchronously pumping a dye laser. This dye laser produces a train of pulses at 82 MHz having pulse energies of $\lesssim 1$ nJ and pulse widths of from 2 to 5 ps depending on the frequency tuning element used. These pulses are propagated through a three-stage dye amplifier which is pumped by the second harmonic of a Q-switched Nd:YAG laser operating at 20 Hz (140 mJ/pulse at 532 nm). The Q switch of the YAG laser is synchronized to the mode-locking frequency synthesizer of the argon ion laser so that a 532 nm pulse and a picosecond pulse arrive at the dye amplifier simultaneously. The overall gain of this amplifier is approximately 1×10^6 yielding a pulse train of visible pulses at 20 Hz which are from 0.5–1.0 mJ/pulse. The temporal shape of the amplified pulses is very similar to that of the input pulses as long as the gain of the amplifier is not much greater than 1×10^6.

As mentioned above, two colors are necessary to perform the pump–probe experiment. In this case, Raman shifting in methane was used to produce a second color. It also serves another purpose and that is to allow the generation of wavelengths blue enough to excite the S_1 state of phenol. The tuning range of the synchronously pumped dye laser extends only to ~ 550 nm, the second harmonic of which, 275 nm, can only excite phenol to the S_1 origin. The anti-Stokes Raman line was used to extend this to higher energies. The output of the amplified dye laser was focused (1 m lens) into a 1 m long high-pressure Raman cell. The light, Raman orders, and fundamental, was recollimated with a 0.5 m lens. Normally to obtain the anti-Stokes shifted UV one would first generate the dye laser second harmonic then use Raman shifting. However, it was found that with these relatively low energy picosecond pulses the second harmonic could not be successfully anti-Stokes Raman shifted. Instead, the fundamental dye laser pulses were scattered in methane ($\Delta\nu = 2914\ \text{cm}^{-1}$) and the first anti-Stokes line was mixed with the fundamental in a KDP crystal immediately after the recollimating lens to obtain the desired UV wavelengths. Best conversion efficiency for mixing was obtained with the recollimating lens close to the output window of the Raman cell as the anti-Stokes radiation diverges, and good overlap with the fundamental is lost quickly as the beams propagate. This mixed frequency UV pulse was then separated from the remaining frequencies and propagated along a fixed optical delay and eventually used for one-photon resonant excitation of the phenol moiety. The remaining frequencies, fundamental, and Stokes-shifted radiation, could be used as the probe. In practice two frequencies were used as the probe: the second harmonic of the dye laser fundamental or the fundamental mixed with the Stokes-shifted light to yield a probe which was further to the red. The generated probe beam was directed to a variable optical delay line which was controlled by a stepper motor driven translation stage. The pump and probe pulses were then recombined on a dichroic mirror so they could be directed to the sample collinearly.

C. The molecular beam and experimental arrangement

The experiment was performed in a supersonic molecular beam which is required to form the van der Waals molecules and as a benefit the internal degrees of freedom in the vdW molecules are extensively cooled resulting in a well defined initial state. The beam apparatus consists of two cham-

bers each of which is pumped by a 6 in. diffusion pump. The first chamber contains a pulsed nozzle which operates at the laser repetition rate, 20 Hz. The nozzle was constructed in our laboratory[16] and can be heated substantially, >250 °C, which is often required for nonvolatile compounds. Under typical operating conditions with 20 psi He behind the nozzle the pressure in this chamber rises to $\sim 2\times 10^{-4}$ Torr. The central portion of the expansion passes through a skimmer, 1.3 mm diam, to the second chamber where the steady state pressure is typically 1×10^{-6} Torr when the valve is in operation.

The laser enters the second chamber perpendicular to the molecular beam and intersects it ~ 10 cm downstream of the nozzle. The intersection of the laser and molecular beam is in the acceleration region of a time of flight mass spectrometer which is similar in design to that of Wiley and McLaren.[17] The drift tube of the mass spectrometer is 3/4 of a meter and contains an ion multipler, EMI 9642/3B, to detect the ions which have been dispersed in time. The arrival of the ions can be recorded by a transient waveform digitizer, Lecroy TR8818, which is based in a CAMAC crate interfaced to an LSI 11/23 + minicomputer. The signal from a number of laser shots can be recorded and averaged in the computer to build up a mass spectrum. In cases where just one mass is to be observed, the output of the ion multiplier is input to a gated integrator/boxcar averager (EG&G 162/164), and the gate positioned to sample the mass peak of interest, with near unit mass resolution in the region of interest.

A pump–probe transient is obtained by sampling the signal in a particular mass channel as a function of the position of the stepper motor controlled optical delay line. This is recorded in a multichannel analyzer whose channel advance is enslaved to the stepper motor driver. The optical delay line can be repetitively scanned for signal averaging.

An experiment was performed in the following way. The wavelength of the transition was obtained from the literature and the laser tuned to this value using a monochromator. Then, using the pump beam alone, the resonance enhanced ionization was maximized to find the transition. The amount of ionization would be reduced to a barely observable level by introducing appropriate neutral density filters. At this point the probe was introduced and the spatial and temporal overlap adjusted to maximize the two laser signal. Enchancements of greater than 3:1 were usually easy to obtain (often >10:1).

Samples were handled as follows. Phenol (Mallinckrodt AR) and cresol (Aldrich $>99\%$) both required heating (60 and 70 °C, respectively) to obtain sufficient densities in the beam so these were introduced into a sample chamber contained in the pulse valve whose temperature could be controlled. The benzene was held in an external vessel through which the He carrier gas flowed and was saturated with the vapor pressure of benzene. Reducing the number of larger clusters $(Ph–Bz)_n$, in the beam was of primary importance so the concentration of benzene was lowered as far as possible without losing all signal from the Ph–Bz species. This was done by maintaining the vessel containing benzene at -45 °C, thereby reducing its vapor pressure to <1 Torr. Ito and co-workers[18] have measured the phenol–benzene spectrum and observed that at benzene pressures of <1 Torr there was almost no signal from the phenol–$(benzene)_2$ species or larger clusters.

III. RESULTS AND DISCUSSION

A. Picosecond transients

The transient behavior of phenol–benzene has been measured for nine vibrational bands. The observed decays

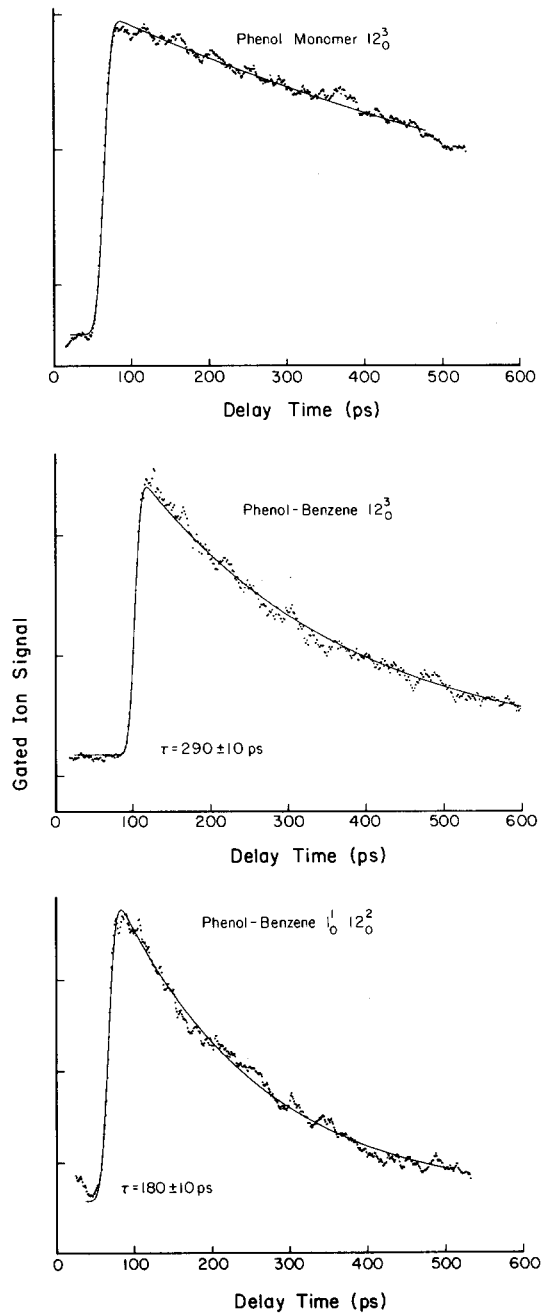

FIG. 3. Phenol–benzene mass-gated ion signal as a function of pump–probe delay time. In the top figure the phenol monomer 12_0^3 resonance (2345 cm^{-1} excess energy) is pumped and signal collected by gating at the monomer mass ($m/e = 94$). The lower two figures were obtained by pumping the phenol–benzene complex (2345 and 2500 cm^{-1}) and collecting signal at the complex mass ($m/e = 172$). A summary of the phenol–benzene data is given in Table I.

TABLE I. Phenol–benzene predissociation rates.

Mode	Energy[a] (cm^{-1})	Δ Energy[b] (cm^{-1})	Rate ($10^9 s^{-1}$)
12_0^2	1564	164	0.42
$1_0^1 12_0^1$[c]	1716	316	0.38
1_0^2[d]	1818	418	1.12
$7a_0^1 12_0^1$	2056	656	2.1
$1_0^1 7a_0^1$	2207	807	3.4
12_0^3	2345	945	3.3
$1_0^1 12_0^2$	2500	1100	5.7

[a] Energy above S_1 origin of phenol.
[b] Energy above the predissociation barrier.
[c] Alternative assignment $4_0^1 10b_0^1 12_0^1$.
[d] Alternative assignment $1_0^1 4_0^1 10b_0^1$.

(Fig. 3) were fit to a single exponential decay with a nonlinear least-squares routine based on the Marquardt algorithm (see paper I). In all cases, a single exponential fit the data (in the time range studied) quite well with little or no improvements being obtained with biexponential fitting. The results are summarized in Table I. As mentioned earlier, several wavelengths were used to probe the reaction but since no difference was observed this will not be referred to in the discussion. The monomer was measured at a number of different excess energies but its decay did not appear to depend sharply on excess energy. Since our accuracy in measuring these longer (ns) lifetimes is limited, these values cannot be usefully quantified but it was clear that they did not decrease significantly at higher energies and so the bare molecule contribution was negligible compared to the complex decay from predissociation.

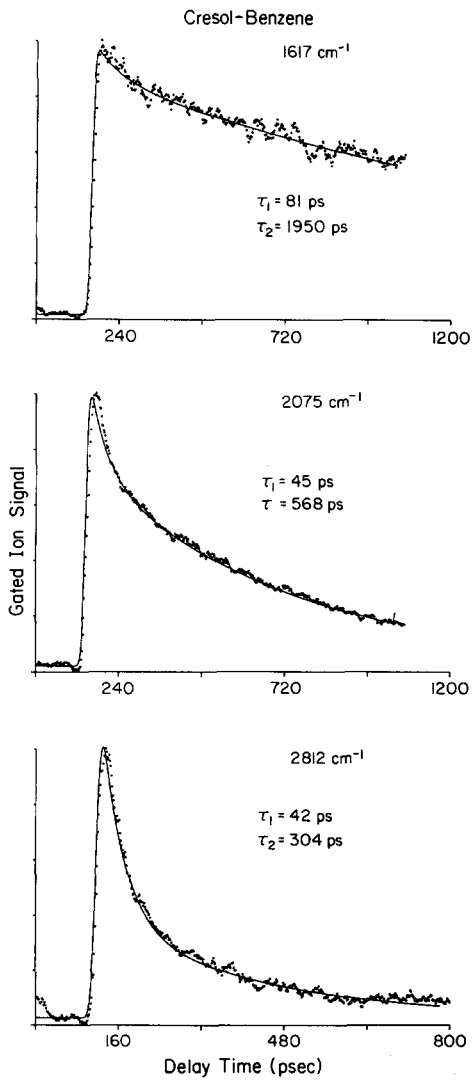

FIG. 4. Cresol–benzene mass-gated ion signal as a function of pump–probe delay time. The lower two transients are clearly biexponential and are representative of the transients obtained above approximately 1700 cm^{-1}. The data for cresol–benzene is summarized in Table II.

TABLE II. Cresol–benzene decay parameters.

Vibrational energy (cm^{-1})	Δ Energy[a] (cm^{-1})	τ_1 (ps)	τ_2 (ps)	Ratio[b]
1617	217	81	1950	0.15
2002	602	46	620	0.38
2075	675	45	568	0.37
2135	735	53	492	0.34
2190	790	46	561	0.48
2420	1020	35	358	0.51
2424	1024	38	266	0.44
2472	1072	34	229	0.44
2635	1235	63	534	0.7
2770	1370	80	690	0.74
2812	1412	42	304	0.70
3195	1795	18	160	0.60

[a] Energy above the predissociation barrier.
[b] Ratio of the fast component intensity to the total signal.

The particular complex transitions studied were chosen because the corresponding monomer bands are known to absorb strongly. The complex bands were found to be shifted $\sim 145\ cm^{-1}$ to the red of the monomer transitions at each of the excess energies studied, in agreement with the value reported by Ito *et al.*[18] for the origin. At low excess energies, distinct resonant enhancements of the complex signal were observed. At higher energies, where the transitions were somewhat weaker and there was considerable spectral congestion, the resonant enhancement was not as distinct. In these cases, the actual wavelength, as measured by a monochromator, was used to tune to the transitions. There were several points taken where the excitation was "off-resonance" meaning excitation into a region where no particularly strong assignable bands were present. No significant deviation was observed from the expected transient behavior for this off-resonant excitation. The highest energy band excited in phenol, 2500 cm^{-1} excess energy, was at the blue limit of the experimentally obtainable wavelengths.

In the cresol–benzene system, 14 vibrational band decays were measured. As can be seen in Fig. 4, at higher energies the transient behavior is no longer a simple exponential. These higher energy transients could be fit well to biexponential decay. In Table II, the data for cresol–benzene is presented with the measured single or biexponential decay constants. For the cases of biexponential decay the contribution of the fast decay component is listed as the ratio of the fast component to the total signal. Again for cresol, a number of measurements were made for the bare molecule at different

excess energies and no dramatic change in rate with excess energy was observed.

B. Structure and spectroscopy

The $\pi\pi^*$ absorption band at 2750 Å of phenol vapor has been analyzed[19] and complexes of phenol with various solvents have been studied previously.[18] Here, we briefly present our studies on the excitation spectrum of *p*-cresol and its complex with benzene.

1. Bare molecule excitation spectrum

The fluorescence excitation spectrum (275–285 nm) of *p*-cresol cooled in a supersonic jet is shown in Fig. 5. The strongest band in the spectrum (35 334 cm^{-1}) is assigned as the electronic origin of the $S_1 \leftarrow S_0$ transition. This corresponds to $\sim 1000\ cm^{-1}$ red shift of the origin as compared to phenol due to 4-methyl substitution and is consistent with shifts on methylation observed in other aromatic molecules.[20] Some of the other bands observed are assigned by comparison with phenol, and we use the notation of Bist *et al.*,[19] namely the same as for benzene. These results are in general agreement with previous analyses of the absorption spectra of the vapor.[21] The 421 cm^{-1} fundamental is a substituent sensitive ring mode ($6a_0^1$). The band at 372 cm^{-1} may be assigned as $16a_0^2$, by analogy with the corresponding band in phenol. It should be noted that the 217 cm^{-1} fundamental assigned by previous authors is not present in this excitation spectrum and should be assigned as a hot or sequence band. The bands having S_1 vibrational energy greater than 700 cm^{-1} reported here correspond to observed resonances closest to those reported by previous authors. These numbers were determined using the picosecond pump–probe apparatus described above. The wavelength obtained for each resonance was converted to absolute wave numbers without vacuum corrections and the value of the S_1 origin subtracted from it to get the relative energies. The assignments for these modes were derived from correlations of published data[21,22] for S_1 and S_0 fundamentals of cresol.

The origin region warrants a careful analysis. The 4-methyl group in toluene is believed to be essentially a free internal rotor.[23] The peaks at 5, 16, and 52 cm^{-1} are very similar to ones observed in the excitation spectrum of jet-cooled toluene and assigned to free internal rotation of the methyl group.[23] These bands derive their intensities from the coupling of internal rotation with overall rotation of the molecule and the band at $-5\ cm^{-1}$ is likely a hot band of this progression. Therefore, this set of bands is probably due to the progression arising from the rotation of the methyl group about the bond connecting it to the aromatic ring.

A low resolution emission spectrum of the vibrationless level of S_1 shows features that may be readily assigned as overtones and combinations of the strongly active 6*a*, 7, and 12 fundamentals.

2. Excitation spectrum of complex with benzene

The ability of aromatic (and olefinic) compounds to form hydrogen bonds with proton donors has been recognized for some time.[24] The spectroscopic studies of Ito and co-workers[18] on 1:1 complexes of phenol with various solvents show a correlation of the shift of the electronic origin and the intermolecular stretching frequencies with thermodynamic data on H-bond strengths. On the basis of comparative evidence, they proposed the structure for the phenol–benzene complex shown in Fig. 1. In this model, OH function points toward the center of the benzene (solvent) ring. Similar data are not available for cresol, but the spectral red shift of the origin and intensity distribution about it are both very similar to the phenol–benzene complex. Since the methyl group is substituted in the *para* position, steric effects are not of importance, and the structure of the complex of benzene with cresol is expected to be the same as with phenol.

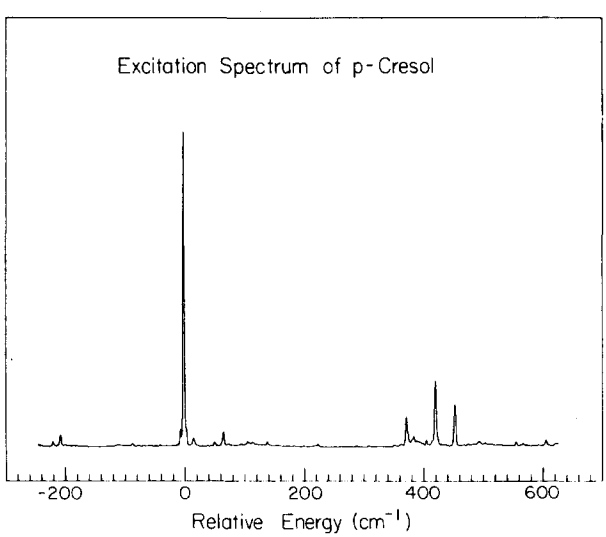

FIG. 5. Fluorescence excitation spectrum of *p*-cresol in a pulsed supersonic jet. The energy scale is referenced to the origin of S_1 in *p*-cresol, 35 334 cm^{-1}.

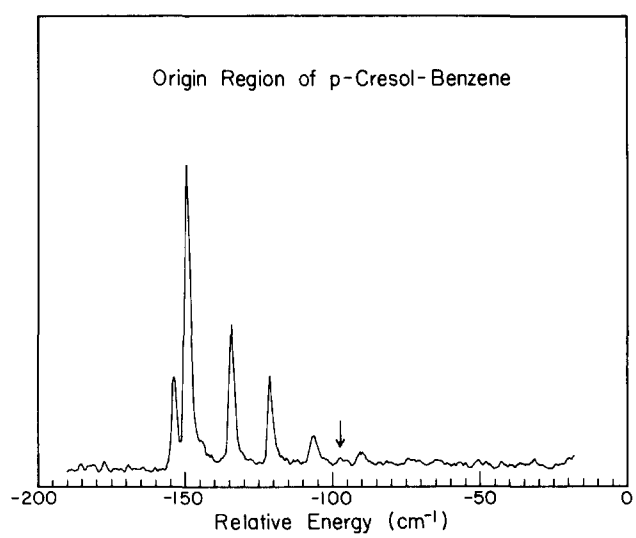

FIG. 6. Fluorescence excitation spectrum of the cresol–benzene van der Waals complex. The energy scale is referenced to the origin of the cresol monomer, 35 334 cm^{-1}. The origin of the complex is ascribed to the largest feature at $-147\ cm^{-1}$. The structure to the blue of the complex origin corresponds to excitation of the intermolecular modes. The arrow marks a feature at $\sim 50\ cm^{-1}$, which is probably the fundamental of the intermolecular stretch.

The excitation spectrum of cresol expanded in Ne saturated with benzene at -15 °C was obtained in the same range as for the bare molecule. Prominent bands showing well-resolved progressions appearing at 35 187 and 35 612 cm^{-1} are assigned to the origin and the $6a_0^1$ transitions of the 1:1 complex respectively. The origin region is shown in greater detail in Fig. 6. The most intense band in this progression is the 0–0 transition shifted 147 cm^{-1} to the red of the origin of free cresol. The set of bands (0, 15, 28, 43, 59) cm^{-1} is tentatively assigned as the progression of an intermolecular bending mode, consistent with a similar progression in the phenol complex. The length of the progression implies a large change in geometry on excitation. Bist *et al.*[19] have shown that the rotational constants of phenol in S_1 are consistent with an increase in the COH bond angle. If this is also true in the case of cresol and complexation with benzene does not affect the equilibrium geometries of the two moieties, a long progression in the "in-plane" intermolecular mode supports the assignment above.

3. Rotational profiles of origin transitions

A high resolution scan of the origin region of cresol shows *P* and *R* branches only. As in phenol, the electronic transition moment is directed along the short in-plane axis, which is also the axis of intermediate moment of inertia of the molecule. Thus the transition is a *B*-type band. A simulation of the rotational profile[25] using structural parameters of phenol for the molecular frame[18] and those of toluene[23] for the methyl rotor agrees well with the measured contour. This comparison is only approximate as the calculations were performed for a rigid molecule of C_{2v} symmetry and the free internal rotation of the methyl group is expected to affect the finer features of the calculations.[26] A similar study of the origin transition of the 1:1 complex shows unresolved *P*, *Q*, and *R* branches. Using the model structure proposed by Ito *et al.*[18] and approximating the H-bond length as the sum[24] of the O–H bond and the half-thickness of the aromatic π-system[27] (crude estimate of the effective van der Waals' radius of benzene), one calculates the principle moments of inertia to be 301(298), 1285(1465), and 1406(1582) amu·Å^2.[28] The numbers in parenthesis are the values for the excited state of the complex. The *a* and *b* principle axes are inclined at $\sim -28°$ to the *y* and *z* axes in the plane of the ring of cresol and the *c* axis is perpendicular to the ring. Thus the excitation in cresol–benzene corresponds to a hybrid band of *A* and *B* types. A simulation of the rotational profile of the complex using these parameters is in qualitative agreement with the measured contour.

The intensity of the band slightly red of the complex origin (-4.5 cm^{-1}) is insensitive to expansion conditions (varying backing pressure from 5–30 psi in different carrier gases) which would suggest that it is not a hot or sequence band. It is possible that this band belongs to the well-developed progression in the bending mode; uneven level spacings have been reported in other molecules with hindered rotors.[20] Abe *et al.*[18] have concluded that a similar pair of closely spaced levels in phenol–benzene are derived from two different conformations. A similar explanation could also be true for the case at hand.

4. Bond dissociation energies

Estimates of the H-bond enthalpy of the phenol complex in the ground state vary from 1.56 to 4.1 kcal/mol. Adiabatic dissociation energies correspond to bond enthalpy at absolute zero and may be derived from enthalpies measured at higher temperatures.[30(a)] The spectral red shift of the S_1 electronic origin implies that the excited state complex is more tightly bound (145 cm^{-1}) than the ground state complex. The reported range of values for the bond enthalpy translates to 875 to 1760 cm^{-1} for the bond dissociation energy in the excited state. Assuming that the transition state involved in the reaction is fairly loose, contribution of tunneling to dissociation rates is negligible. Our experiments therefore show that the energetic threshold to dissociation lies between 1250 and 1550 cm^{-1}, which is well within the range quoted in the literature. In all discussions below, we choose 1400 cm^{-1} as the van der Waals' bond energy for Ph–Bz.

No measured values of the bond enthalpy for cresol–benzene are available, but estimates may be derived from comparisons of systems involving phenol or cresol with a common solvent. The free energies of complexation of phenol and cresol with benzene differ by $\sim$0.05 kcal/mol ($\sim$20 cm^{-1}).[30(b)] Assuming the entropy change is the same in each case, the H-bond energies of the two compounds should account for the difference in free energies. The dissociation energy of the cresol–benzene complex is therefore chosen to be the same as that of Ph–Bz, i.e., $\sim$1400 cm^{-1}. This choice is also supported by the spectral red shift in the cresol complex, 147 cm^{-1}, provided the correlation with bond energies is valid.

C. Ionization and electronic state dynamics

The question of how the observed decays are ascribed to vibrational predissociation from the S_1 state of phenol is addressed first. Typical transient ion signals are shown in Fig. 3. In the lower transient the initial excitation is 2500 cm^{-1} above the phenol origin, which should be safely above the predissociation barrier estimated to be approximately 1400 cm^{-1}. In this figure, the ion signal of the mass corresponding to phenol–benzene is plotted as a function of pump–probe delay time. At the same excess energy the phenol monomer lifetime is considerably longer, $\sim$2 ns, indicating that the fast decay is associated with dynamics which occur only in the complex. The approximately 2 ns decay is the excited electronic state lifetime. The most straightforward interpretation is that the complex is predissociating in the neutral molecule causing a loss of signal from the Ph–Bz complex mass channel. A conclusive check of this would be the observation of a corresponding rise in intensity in the phenol monomer mass channel as the reaction proceeds because the dissociated phenol fragment remains electronically excited and should absorb the probe to give monomer ions. Unfortunately this was not possible because a large background of monomer ions was found to be always present. It comes from two sources. First, the absorption by phenol monomer molecules at the wavelength where the complex absorbs. Even though the resonance favors the complex there is a much greater concentration of monomers and particularly at higher ener-

gies there are always small absorption features present even in the cold supersonic beam. Second, there is contribution to the monomer ion channel from fragmentation of the complex ions. $[Ph–Bz]^+ \rightarrow Ph^+ + Bz$. This occurs because the probe excites the complex 7285 cm^{-1} above the ionization threshold,[31] certainly exceeding the complex ion binding energy. The ionization process results in a distribution of ion vibrational states determined by Franck–Condon factors (as would be observed in the photoelectron spectrum) leaving some complex ions above the dissociation barrier and others below it. This determines the fraction of complex ions which dissociate and it appears from our observations that a substantial amount do fragment. It should be emphasized that these dissociation processes cannot contribute to the observed dynamic behavior because ionization occurs after the absorption of two photons and thus any post ionization events are independent of pump–probe delay time.

There are several alternative explanations of the observed decay which have been considered and can be shown to be improbable. One possibility is that the observed decay is due to intramolecular vibrational energy redistribution of the initially prepared well defined vibrational state. It might be argued that the initially prepared state has a larger cross section for ionization than the redistributed states thereby leading to a decrease in the ionization signal as population goes into the redistributed states.[15(a)] One simple argument against this is that uncomplexed phenol does not exhibit this type of behavior even at the maximum excess energy studied, 2500 cm^{-1}. Of course it is possible that the presence of the van der Waals bond could induce IVR at a lower excess energy. One must then consider the specifics of what the cross section for ionization should be for one vibrational state vs another. The ionization cross section is the product of the electronic transition moment between S_1 and the ion ground state, the vibrational Franck–Condon factors and an electron continuum function. The effect of the Franck–Condon factors may give rise to a difference in cross section from one S_1 vibrational state to another, which will depend on the probe photon wavelength. If one probes near the ion threshold only some vibrational states of the ion will be accessible and these will determine the Franck–Condon factors. On the other hand, when one excites substantially above the ionization threshold all the ion vibrational states become accessible. In this case, the ionization cross section becomes the same for all vibrational states because the integrated F–C factors from any one vibrational state to all other states in another electronic manifold are equal. So when one is exciting sufficiently above the ionization threshold the behavior can be compared to that of a fluorescence spectrum in this regard. In the experiments on phenol and cresol several probe wavelengths were used to investigate the effect, if any, of the probe photon energy on the transient behavior of the complexes. The redder probe excited to approximately 4370 cm^{-1} above the threshold while the blue probe was 7285 cm^{-1} above it, certainly well beyond the point at which there might be increasing intensity due to F–C overlap with highly excited ion vibrational states. Transients obtained using either probe wavelength showed identical behavior suggesting that the decay in the ionization signal was not due to vibrational redistribution in the neutral molecule.

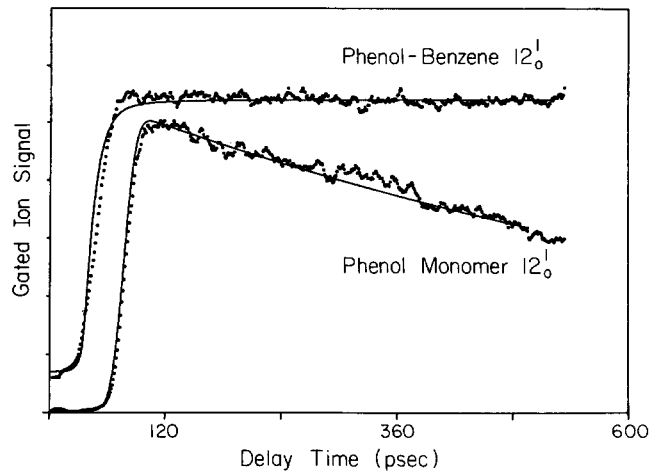

FIG. 7. Comparison of the transient behavior of the phenol monomer to that of the phenol–benzene complex when pumping the 12_0^1 transition (782 cm^{-1}). The population is monitored by ionizing the intermediate state with a probe pulse and measuring the mass-gated ion signal, $m/e = 94$ for phenol and $m/e = 172$ for the complex.

Another possible explanation for the observation of decay in the phenol–benzene complex is that some nonradiative electronic decay is induced by the presence of the van der Waals partner. Quantum yield and absorption measurements of phenol in solution[32] showed that in cyclohexane the S_1 state of phenol has a fluorescence lifetime of ~ 2 ns and a quantum yield of 0.08, whereas in methanol the lifetime is lengthened considerably to 7 ns with a quantum yield of 0.22. This should be compared to our measurements of the lifetime of phenol and phenol–benzene complexes near the origin of S_1 where no vibrational predissociation occurs. As can be seen in Fig. 7, the phenol monomer has a lifetime of 1 to 2 ns (the picosecond system is set up for measurement of short time intervals and cannot accurately measure lifetimes greater than 1 ns) while the complex is showing essentially no decay on our time scale and must have a lifetime > 5 ns. There is some mechanism, electronic or vibrational,[33] which is reducing the nonradiative decay in the complex. These observations are consistent with earlier work on hydrogen bonding of water and alcohol with isoquinoline.[9] This suggests that the interactions observed in the isolated van der Waals species are similar to those present in solution, supporting the idea presented above that the structure of phenol–benzene is a π hydrogen bonding interaction. The point is that the formation of the van der Waals bond actually inhibits nonradiative decay and it is unlikely that this changes dramatically with excess energy to the point where nonradiative decay is much faster than in the monomer.

Further evidence that vibrational predissociation is being measured comes from the observation of rates vs excess vibrational energy. First, the onset of measurable decay in the phenol–benzene complex is between 1275 cm^{-1}, where no decay is observed, and 1564 cm^{-1} which is the first complex band to decay appreciably. The observed threshold behavior agrees with the thermodynamic data, as discussed above. Second, the trend of the rates is also consistent with a

predissociation process. RRKM calculations presented below show the same trend as the measured dissociation rates of the phenol–benzene system. To summarize, there is substantial evidence that vibrational predissociation is being directly measured in the phenol–benzene system and by analogy in cresol–benzene as well.

D. Phenol–benzene predissociation

The single exponential decay constants observed for the phenol–benzene species are listed in Table I and plotted as a function of excess vibrational energy in Fig. 8. As discussed above, the decay mechanism has been ascribed to vibrational predissociation so the excess energy scale is relative to the reaction threshold. From examining Fig. 8, one can see that the rates are following a consistent trend—increasing predissociation rate as a function of excess energy. This is to be expected if the reaction is statistical, i.e., the initially deposited energy is completely randomized prior to reaction. The question now is are there any mode specific effects which would show unexpected behavior in the trend of the rates. Data points showing marked deviation from the trend or an irregular distribution of rates with no clear excess energy dependence would imply that the dynamics include nonstatistical effects. There are several data points which do not follow the trend exactly, in particular the decay at 1818 cm^{-1} (i.e., 418 cm^{-1} above threshold), which is decidedly biexponential, but these are fairly small deviations and given the confidence limits one has to conclude that there are no obvious mode specific effects. Subtle effects may be present but cannot be asserted with the present data set. The question now is: What is the degree of statistical behavior among modes in the complete vibrational phase space?

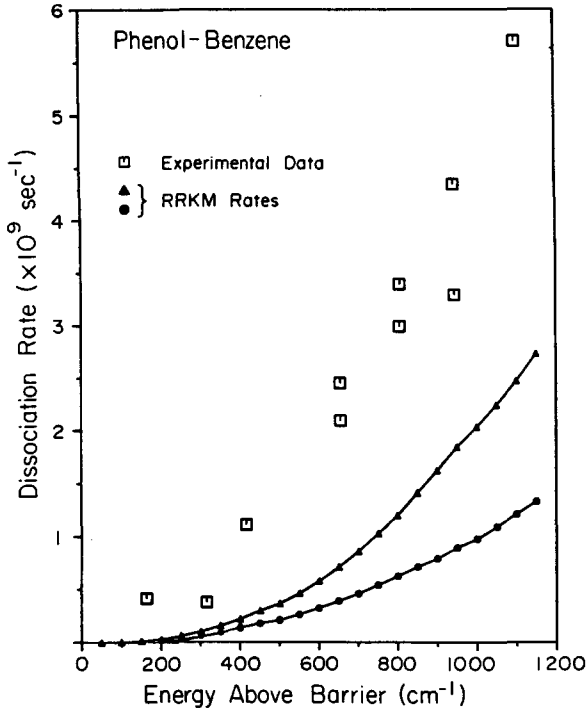

FIG. 8. Plot of the vibrational predissociation rates of the phenol–benzene van der Waals molecule as a function of excess energy above the dissociation threshold, 1400 cm^{-1}. The squares are the rates from a single exponential fit of the experimentally measured decay curves. The plotted data includes results from our earlier work (Ref. 13) as well as more recent results. The triangles are the rates obtained using standard RRKM calculations on the phenol–benzene system with the exclusion, however, of the benzene vibrational frequencies. The circles are the same calculation including the benzene modes. See the text for details of the calculations.

Since phenol–benzene must dissociate following energy redistribution, we chose to model the rates using standard routines[34] based on RRKM theory. A PST calculation (see papers I and II) is perhaps more appropriate since we expect the TS to be fairly loose, but we do not attempt it here. The purpose of these calculations is to see if the order of magnitude of the observed rates can be reproduced and if the trend is as expected. In order to do a meaningful calculation, all the vibrational frequencies in the molecule must be known as well as the frequencies of the transition state. In a system the size of phenol–benzene this is obviously difficult particularly because the intermolecular modes, van der Waals bond stretch, four bends and a free or hindered rotation, are difficult to determine accurately. Fortunately, two of the intermolecular modes, the vdW stretch and one of the bends, have been observed spectroscopically for phenol–benzene, 50 and 20 cm^{-1}, leaving only four others to be estimated. The modes for phenol have been determined almost completely and so are not a problem. As alluded to in the introduction, the constituent molecules of the complex are not highly excited by the energy deposited to break the van der Waals bond and thus anharmonic corrections for these modes are relatively unimportant and were not included in the calculation. We assume that in the transition state, the vibrational frequencies of the constituent molecules change very little because the breaking of the weak van der Waals bond is only a small perturbation. However, our poor knowledge of the intermolecular modes means that a rigorous calculation is not possible. As a first attempt a standard RRKM calculation was performed in which the frequencies of the transition state were chosen to be the same as in the reactant molecule. Reasonable values were chosen for the intermolecular modes and the calculation (for adiabatic rotations, i.e., counting vibrational density of states only) performed without adjusting any of the parameters to fit the data. This should give an estimate of the reaction rates and their excess energy dependence without a bias from adjusting parameters. One point which needs to be addressed is whether or not the benzene vibrational modes play a role in the dynamics, i.e., does vibrational energy transfer across the weak vdW bond to the benzene in the IVR process. It seems rather unlikely that the energy necessary to excite the relatively high frequency modes of the benzene moiety would transfer efficiently across the weak vdW bond, but as a check the calculation was done with and without these modes. The results of the calculations are shown in Fig. 8 where RRKM rates are plotted with experimental results for phenol–benzene. A much better fit of the data is obtained if the transition state is made somewhat loose by decreasing the frequencies of the intermolecular modes by 20%. A loose transition state is certainly expected in this case as there should be no appreciable barrier to dissociation in the long range attractive van der Waals' potential. The important point is that the trend in the experimental rates can be reproduced by the

calculation, which implies fast energy redistribution. However, energy redistribution is not necessarily complete and this may account for deviations (observed rates faster than calculated ones). Since the energy is being deposited selectively through optically active transitions, IVR must be occuring on a time scale fast compared to the predissociation process but to a subset of states in the vibrational phase space. Unfortunately the calculations are not accurate enough e.g., to determine if the benzene modes are involved except to show that in the standard RRKM calculation inclusion of these modes gives results that are even further from the experimental results than without them.

The phenol–benzene system can now be used as a point of reference for comparison to the behavior of substituted phenol–benzene vdW molecules. The idea is that although the RRKM calculations might be subject to problems in calculating the absolute rates and the degree of statistical behavior they should be quite accurate for relative rates between similar systems particularly where the unknown quantities, vdW mode frequencies, are the same in each system. The system used for comparison is cresol–benzene, where a methyl group is "added" to the phenol–benzene complex.

E. Cresol–benzene predissociation

In the cresol–benzene system, some evidence of decay is seen below the barrier that was chosen (*vide supra*) which is probably due to fluorescence from the complex (ns). The decays at ~ 1200 cm^{-1} are dominantly single exponential with some hint of a faster process. At low energies, the fast component is only a small fraction of the total signal. Limited signal-to-noise and fluctuations during signal averaging makes it difficult to make any strong assertions at these energies. As the excess energy above the barrier is increased, a biexponential fit of the transient becomes signficantly better than a single exponential one and the fast component of the decay becomes a larger fraction of the total signal. (In fact the ratio of the fast component to the total signal, Table II, is one of the most predictable variables of the excess energy; it increases systematically with almost no deviations).

The lifetime of the fast component does not show a regular trend with excess energy but instead appears to fluctuate. The long component of the decay shows a more regular trend—decreasing lifetime with increasing excess energy but these values also fluctuate at higher energies. The origin of this biexponential behavior as compared to the apparently simple behavior of phenol is addressed below.

There is spectroscopic evidence of at least two different conformations of the Ph–Bz[18] complex which raises the possibility that for cresol–benzene two conformations, with different decay rates, are responsible for the biexponential behavior. If there are two types of binding sites for the benzene, each with its own barrier, the observed signal will be the sum of two individual ensembles of complexes. In order to account for the observed behavior, one has to assume that the complexes which give rise to the fast component have a much lower barrier and are not formed with phenol. A number of observations argue strongly against this as the source of the measured biexponentials. First, the fast component does not appear until 1617 cm^{-1} which is the opposite of what would be expected for a complex with a lower barrier. Secondly, the fast component does not show an excess energy dependence that would be indicative of a simple additional contribution from a separate ensemble of complexes. Finally, there does not seem to be a change in the ratio of the fast to slow components by tuning on and off known complex resonances which should favor one ensemble of complexes over another.

Next we consider the behavior of a complex with one well defined structure. The appearance of more complicated decay behavior is then indicative of several competing processes which contribute to the experimental observations. These might be processes such as intramolecular vibrational redistribution or interelectronic nonradiative decay which do not directly involve dissociation but can lead to a loss of observed signal due to decreased ionization probabilities from the redistributed (dark) states. This point was addressed in some detail above in ascribing any decay to dissociation and the arguments against these mechanisms are just as valid for cresol–benzene dissociation. One cannot rule out the possibility that these processes are occurring, especially since in the case of phenol–benzene there is at least some IVR prior to dissociation. If this redistribution process is very fast compared to dissociation then no evidence for it will be observed in the transient decay (as in the Ph–Bz case). Energy redistribution processes occuring on timescales comparable to the dissociation rate can show multiexponential decay behavior if the initial and redistributed states have different dissociation rates. This situation would exclude the use of simple statistical models which require total redistribution to be fast compared to any dissociation process. The data for cresol–benzene is indeed biexponential, and in the model presented below we discuss our results taking into account energy redistribution prior to vibrational predissociation. Certainly other, more complicated, models can be introduced but the point here is to show how these competing processes can lead to the observation of biexponential decays. The possible nature of state distributions before and after this redistribution process will then be discussed.

F. Energy redistribution and vibrational predissociation

The model which we have used (see also papers I and II) to describe the cresol–benzene decay is as follows. The pump pulse initially prepares a state(s), $\{|s\rangle_i\}$, which has two nonradiative channels open to it. One of the channels is vibrational predissociation which results in a decrease in the experimentally observed signal. The second channel is energy redistribution to isoenergetic states of the complex, denoted by $\{|l\rangle_i\}$. The states $\{|l\rangle_i\}$ also have a vibrational predissociation channel open. The kinetic scheme is

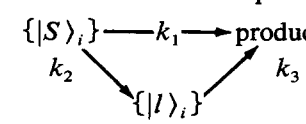

The validity of a kinetic model for describing dissociation has been considered in paper I, and here we ignore coherence effects and reversible processes for reasons discussed earlier

in papers I and II. The concept of dividing the phase space to account for biexponential decay kinetics follows from previously described models of IVR[15(a)] and non-RRKM behavior.[35]

As was mentioned before, we expect that vibrationally redistributed states, $\{|l\rangle_i\}$, have the same cross section for ionization as the initial states, $\{|s\rangle_i\}$ (because of the energetics of the experiments), and thus the observed signal will not reflect the population in $\{|s\rangle_i\}$ but will rather give the sum of population in $\{|s\rangle_i\}$ and $\{|l\rangle_i\}$. Therefore, to model the experimental observable kinetic equations are solved for the quantity $[\{|s\rangle_i\}+\{|l\rangle_i\}]$, which yields

$$[\{|s\rangle_i\}+\{|l\rangle_i\}] = \frac{I_0}{k_1+k_2-k_3}\left[(k_1-k_3)e^{-(k_1+k_2)t}+k_2e^{-k_3t}\right].$$

The experimental measurements on cresol–benzene dissociation at higher energy can be fit with a biexponential decay which yields three unique parameters. The time-dependent signal, $I(t)$, is given by

$$I(t) = Ae^{-\alpha t} + Be^{-\beta t},$$

where the fast component decay rate is α, the slow component decay rate is β, and the ratio of the fast component to the total signal, $F_A = A/(A+B)$. These experimentally observed quantities can be related to the kinetic model parameters as follows:

$$k_1 = F_A(\alpha-\beta)+\beta,$$
$$k_2 = \alpha - k_1 = (\alpha-\beta)(1-F_A),$$
$$k_3 = \beta.$$

Thus, within the limits of this model one can identify the predissociation rates from the initial states k_1, the redistribution rate to $\{|l\rangle_i\}$, k_2, and the predissociation rate from the $\{|l\rangle_i\}$ states k_3. The physical rationale behind this model can now be investigated to see if the results obtained appear reasonable. First, the nature of the initial states, $\{|s\rangle_i\}$ must be addressed. By analogy to phenol–benzene one would expect there to be a redistribution process which is fast compared to dissociation. Therefore it is likely that the initial state in the kinetic model $\{|s\rangle_i\}$ is not the optically prepared state but some set of states formed by an initial rapid (much faster than dissociation) redistribution. Competing with predissociation (k_1) would be redistribution to available bath states of the complex $\{|l\rangle_i\}$ with a rate constant k_2. These redistributed states dissociate more slowly, k_3, in this model (see below).

The exact nature of the division of the vibrational phase space is difficult to ascertain. Here, we consider two cases. First, we consider case (a), where k_1 is the dissociation rate from the initial, partially randomized, set of states, k_2 is the slower redistribution rate which populates the entire phase space, and k_3 is the predissociation rate from this distribution. As can be seen from Table III the values for k_1 and k_2 vary considerably and do not show a regular trend. This is understandable if one examines the expressions for k_1 and k_2. They depend on all three experimental parameters, α, β, and F_A, in a complicated way and the experimental uncertainties are compounded. The predissociation rate k_3 is directly measured experimentally as β, the long-component of the biexponential decay and should, therefore, be a more reliable figure. Accordingly, k_3 is the decay rate from the "equilibrated" phase space of the cresol–benzene, $\{|l\rangle_i\}$, which is consistent with the predictions of the models in Refs. 15(a) and 35. If this is the case, then the RRKM calculations should yield k_3. As mentioned earlier, we can use the relative RRKM calculations obtained to fit the phenol–benzene complex decay and modify it by just including the additional methyl vibrational modes. The barrier and other modes, including those of the transition state, are assumed to be the same. The results of this calculation are plotted in Fig. 9 along with the experimentally obtained values of k_3. Although the calculations do seem to give the average trend, there is definite deviations in the experimental data around the RRKM curve. In case (b), we consider the $\{|l\rangle_i\}$ states to represent bath modes of the methyl group. Accordingly, k_3 is the predissociation rate from the bath states and again they should be slower than k_1+k_2. The biexponential behavior in cresol–benzene is therefore reflecting phenol–benzene behavior in addition to predissociation from physically remote methyl bath modes. More experiments involving partial deuteration and longer alkyl chains (or other substituents) would be of extreme interest to learn about the nature of vibrational energy redistribution in these prototype systems.

TABLE III. Cresol–benzene kinetic model rates.

Vibrational energy (cm^{-1})	Δ Energy[a] (cm^{-1})	$k_1\times10^9$ (s^{-1})	$k_2\times10^9$ (s^{-1})	$k_3\times10^9$ (s^{-1})
1617	217	2.3	10.1	0.5
2002	602	9.3	12.5	1.6
2075	675	9.3	12.9	1.8
2135	735	7.8	11.1	2.0
2190	790	11.4	10.4	1.8
2420	1020	15.9	12.6	2.8
2424	1024	13.7	12.6	2.8
2472	1072	15.4	14.0	4.4
2635	1235	11.7	4.2	1.9
2770	1370	9.6	2.9	1.5
2812	1412	17.6	6.2	3.3
3195	1795	11.4	10.4	1.8

[a] Energy above the predissociation barrier.

G. Homogeneous linewidth and VP rates

As mentioned in papers I and II, in large molecular systems one must be careful in relating the apparent linewidth to IVR and VP dynamics. The present study indicates that the contribution of VP/IVR rates to the homogeneous linewidth is 0.01 to 0.1 cm^{-1}, (the apparent rotational contour is, of course, much larger than this value) above the barrier to dissociation. Below the barrier, the width is less, being $\sim$0.005 cm^{-1}. It would be interesting to perform high-resolution contour analysis on these systems below and above the barrier and compare with time-resolved data reported here.

The biexponential behavior reported here is different

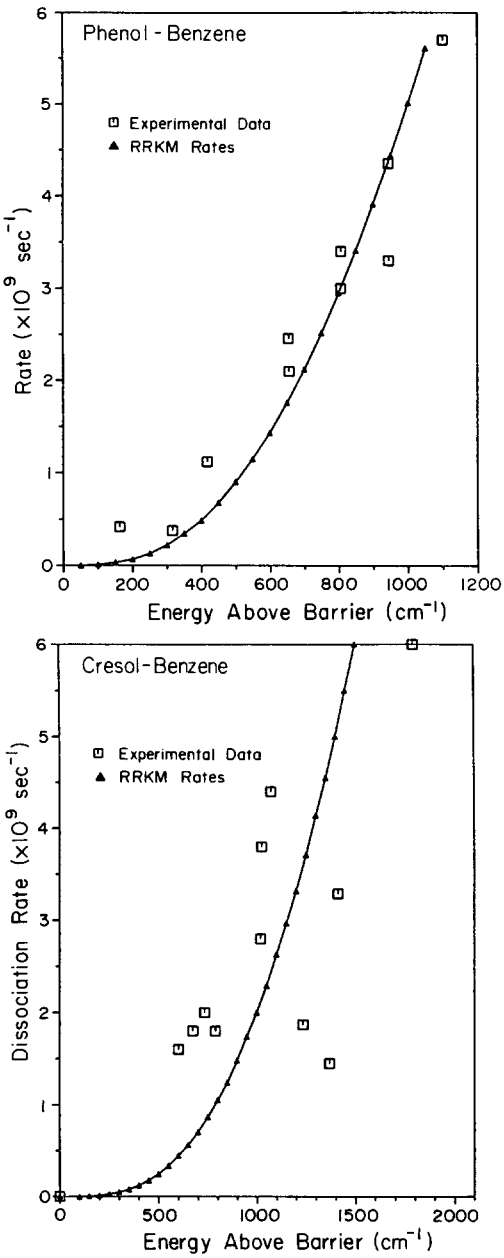

FIG. 9. Comparison of experimental rates to adjusted RRKM rates. The upper half shows the observed rates and calculations for the phenol–benzene complex, while the lower one shows the same for the complex of cresol. Calculated rates are for a transition state with frequencies 20% smaller than in the reactant and are plotted as a solid line. The fundamental frequencies for cresol were chosen to be the same as the corresponding ones in phenol, augmented by those for a methyl substituent. See the text for further details.

from that observed in gaseous benzene in the channel 3 region. As discussed elsewhere,[7,36] thermal congestion can lead to inhomogeneous superposition of transitions and to biexponential decay. In our case, the system is cooled by supersonic-beam expansion and inhomogeneous vibrational excitations are essentially eliminated. Inhomogeneous rotational excitation could, however, be significant. If there were a strong rotational dependence for VP, nonexponential decays would be observed even in a beam experiment.

A final comment regarding VP rates is now made. Throughout the paper we compared our experimental results with RRKM rates. In the literature,[37] the classical RRK expression was used to describe VP of van der Waals molecules. The argument applied to the system *n*-octylbenzene–Ar was as follows. Using the classical RRK expression

$$k = A\left(1 - \frac{E_0}{E}\right)^{s-1}$$

the prefactor A was estimated to be $\sim 10^{13}\text{s}^{-1}$ and $s = 24$ to obtain $k \approx 0.1\ \text{s}^{-1}$—ten orders of magnitude slower than the inferred experimental rate. The author used this large disparity to claim deviation from statistical behavior. However, as discussed in this paper, the RRKM theory (semiclassical) is more appropriate for comparing with experiment than the classical RRK theory.

IV. CONCLUSIONS

This paper, the third in the series, presents picosecond time-resolved fragmentation of van der Waals clusters. Using a picosecond pump–probe mass-spectrometry technique, we have measured the dissociation rates for the weakly bound beam-cooled systems phenol–benzene and cresol–benzene. Excitation was to specific vibrational states in the S_1 state of phenol (cresol) and dissociation proceeds on this electronic surface.

The main findings are:

(a) for the case of phenol–benzene the rates of dissociation increased smoothly with increasing excess energy. The trends could be modeled using simple RRKM calculations although restricted IVR is also included.

(b) The cresol–benzene system showed markedly different behavior, exhibiting *biexponential* decays as the energy is increased above reaction threshold. This we describe using a model for partitioning phase space, with each part exhibiting its own dissociation rate. At least partial energy redistribution occurs prior to vibrational predissociation.

(c) The binding energy of benzene to phenol is $\sim 1400\ \text{cm}^{-1}$, as measured from rates vs excess energy, and dissociation contributes at most $0.1\ \text{cm}^{-1}$ to homogeneous broadening above threshold.

Picosecond photofragment spectroscopy using photoionization mass spectrometry or LIF techniques should be general for studying a large number of dissociation reactions, including other van der Waals clusters. Our current apparatus (see papers I and II) offers independent tunability for both pulses, and this provides additional sensitivity for probing the dynamics of recoil as a function of energy in the reagent or fragments.

Note added in proof: Using fluorescence detection, mode-selective (non-RRKM) behavior have been observed recently for the vdW system stilbene–He. For more details see: D. Semmes, J. S. Baskin, and A. H. Zewail, J. Am. Chem. Soc. (in press).

ACKNOWLEDGMENT

This work was supported by a grant from the National Science Foundation (DMR 85-21191).

[1](a) For reviews see: D. H. Levy, in *Photoselective Chemistry*, edited by J. Jortner, R. D. Levine, and S. A. Rice (Wiley, New York, 1981), part 1, p.

323. (b) J. A. Beswick and J. Jortner, Ref. 1, p. 363. (c) K. C. Janda, Adv. Chem. Phys. **60**, 201 (1985).
[2]R. E. Smalley, D. H. Levy, and L. Wharton, J. Chem. Phys. **64**, 3266 (1976).
[3]See, e.g., (a) D. V. Brumbaugh, J. E. Kenny, and D. H. Levy, J. Chem. Phys. **78**, 3415 (1983). (b) C. A. Hayman, D. V. Brumbaugh, and D. H. Levy, J. Chem. Phys. **81**, 2282 (1984). (c) T. A. Stephenson and S. A. Rice, *ibid.* **81**, 1083 (1984). (d) N. Halberstadt and B. Soep, Chem. Phys. Lett. **87**, 109 (1982). (e) A. Amirav, U. Even, and J. Jortner, J. Chem. Phys. **25**, 2489 (1981). (f) J. Wanna and E. R. Bernstein, *ibid.* **84**, 927, 1981; K. S. Law and E. R. Bernstein, *ibid.* **82**, 2856 (1985), and references therein.
[4]See, e.g. (a) A. Mitchell, M. J. McAuliffe, C. F. Giese, and W. R. Gentry, J. Chem. Phys. **83**, 4271 (1985). (b) M. P. Casassa, D. S. Bomse, and K. C. Janda, *ibid.* **74**, 5044 (1981). (c) G. T. Fraser, D. D. Nelson, A. Charo, and W. Klemperer, *ibid.* **82**, 2535 (1985). (d) A. S. Pines and W. J. Lafferty, *ibid.* **78**, 2154 (1984). (e) T. E. Gough, R. E. Miller, and G. Scoles, *ibid.* **69**, 1588 (1985). (f) D. S. King and J. C. Stephenson, *ibid.* **82**, 5286 (1985). (g) For a recent review, see R. E. Miller, J. Phys. Chem. **90**, 3301 (1986).
[5]A. H. Zewail, Acct. Chem. Res. **13**, 360 (1980).
[6]See, e.g., M. J. Burns, W. K. Liu, and A. H. Zewail, in *Spectroscopy and Excitation Dynamics of Condensed Molecular Systems*, edited by V. M. Agranovish and R. M. Hochstrasser (North-Holland, New York, 1983), Vol. 4.
[7]A. H. Zewail, Ber. Bunsenges. Phys. Chem. **89**, 264 (1985); R. Gentry, in *NATO Advanced Research Workshop*, edited by A. Weber (Reidel, Dordrecht, 1987).
[8]P. M. Felker and A. H. Zewail, in *Applications of Picosecond Spectroscopy to Chemistry*, edited by K. B. Eisenthal (Reidel, Dordrecht, 1983), and references therein.
[9]P. M. Felker and A. H. Zewail, Chem. Phys. Lett. **94**, 454 (1983); J. Chem. Phys. **78**, 5266 (1983).
[10](a) J. F. Ramaekers, J. Langelaar, and R. P. H. Rettschnick, in *Proceeding of the Third International Conference on Picosecond Phenomena* (Springer, Berlin, 1982). (b) J. F. Ramaekers, L. B. Krijnen, H. J. Lips, J. Langelaar, and R. P. H. Rettschnick, Laser Chem. **2**, 125 (1983). (c) M. Heppener, A. G. Kunst, D. Bebelaar, and R. P. H. Rettschnick, J. Chem. Phys. **83**, 5341 (1985).
[11]D. D. Smith, A. Lorincz, J. Siemon, and S. A. Rice, J. Chem. Phys. **81**, 2295 (1984).
[12](a) J. S. Baskin, P. M. Felker, and A. H. Zewail, J. Chem. Phys. **84**, 4708 (1986); J. S. Baskin, D. H. Semmes, and A. H. Zewail, *ibid.* **85**, 7488 (1986). (b) D. H. Semmes, J. S. Baskin, and A. H. Zewail (to be published).
[13]J. L. Knee, L. R. Khundkar, and A. H. Zewail, J. Chem. Phys. **82**, 4715 (1985).
[14]L. R. Khundkar, J. L. Knee, and A. H. Zewail, J. Chem. Phys. **87**, 77 (1987), paper I in this series. (b) N. F. Scherer and A. H. Zewail, J. Chem. Phys. **87**, 97 (1987), paper II in this series.
[15](a) J. W. Perry, N. F. Scherer, and A. H. Zewail, Chem. Phys. Lett. **104**, 1 (1983); N. F. Scherer, J. W. Perry, F. E. Doany, and A. H. Zewail, J. Phys. Chem. **89**, 894 (1985). (b) J. L. Knee, L. R. Khundkar, and A. H. Zewail, *ibid.* **89**, 3201 (1985). (c) J. L. Knee, F. E. Doany, and A. H. Zewail, J. Chem. Phys. **82**, 1042 (1985). (d) J. L. Knee, L. R. Khundkar, and A. H. Zewail, *ibid.* **83**, 1996 (1985).
[16](a) B. W. Keelan, J. A. Syage, J. F. Shepanski, and A. H. Zewail, in *Proceedings of the International Conference on Lasers* (STS, Mclean, VA, 1985), p. 718. (b) B. W. Keelan and A. H. Zewail, J. Chem. Phys. **82**, 3011 (1985).
[17]W. C. Wiley and I. H. McLaren, Rev. Sci. Instrum. **26**, 1150 (1955).
[18](a) H. Abe, N. Mikami, and M. Ito, J. Phys. Chem. **86**, 1768, (1982). (b) H. Abe, N. Mikami, M. Ito, and Y. Udagawa, **86**, 2567 (1982). (c) Chem. Phys. Lett. **93**, 217 (1982). (d) A. Oikawa, H. Abe, N. Mikami, and M. Ito, J. Phys. Chem. **87**, 5083 (1983).
[19](a) H. D. Bist, J. C. D. Brand, and D. R. Williams, J. Mol. Spectrosc. **21**, 76 (1966). (b) H. D. Bist, J. C. D. Brand, and D. R. Williams, J. Mol. Spectrosc. **24**, 413 (1967).
[20]J. A. Syage, P. M. Felker, D. H. Semmes, F. al Adel, and A. H. Zewail, J. Chem. Phys. **82**, 2896 (1985).
[21](a) S. Imanishi and M. Ito, Bull. Chem. Soc. Jpn. **25**, 153 (1952). (b) P. R. Rao, Proc. Ind. Acad. Sci. Sect. A **55**, 232 (1962).
[22]R. J. Jacobsen, Spectrochim. Acta **21**, 433 (1965).
[23]H. D. Rudolph, H. Driezler, A. Jaeschke, and P. Wendling, Z. Naturforsch. Teil A **22**, 940 (1967). (b) J. Murakami, M. Ito, and K. Kaya, Chem. Phys. Lett. **80**, 203 (1981). (c) M. Ito, J. Phys. Chem. **91**, 517 (1987).
[24]G. C. Pimentel and A. I. McClellan, in *The Hydrogen Bond* (Freeman, San Francisco, 1960).
[25]Ref. 16(b); H. Selzle, W. E. Howard, and E. W. Schlag, *Rotational Band Contour Program* (Technische Universität, München), (implemented on a VAX 11/780).
[26](a) T. Cvitas and J. M. Hollas, Mol. Phys. **20**, 645 (1971). (b) T. Cvitas, J. M. Hollas, and G. H. Kirby, *ibid.* **19**, 305 (1970).
[27]*Handbook of Physics and Chemistry*, edited by P. Weast, 60th ed. (Chemical Rubber, Boca Raton, FL, 1980).
[28]The eigenvalues of the inertia tensor were obtained from the cubic characteristic equation using Cardan's formulas. The eigenvectors were obtained numerically using iterative deflation with orthogonalization in each iteration.
[29](a) D. Werst, R. Gentry, and P. Barbara, J. Phys. Chem. **89**, 730 (1985). (b) L. R. Khundkar and A. H. Zewail, J. Chem. Phys. **86**, 1302 (1986).
[30](a) L. R. Khundkar, R. A. Marcus, and A. H. Zewail, J. Chem. Phys. **87**, 2473 (1983). (b) D. Blaser, J. Murphy and J. N. Spencer, Can. J. Chem. **49**, 3913 (1971); Z. Yoshida and N. Ishiba, Bull. Chem. Soc. Jpn. **42**, 3254 (1969).
[31]N. Gonohe, H. Abe, N. Mikami, and M. Ito, J. Phys. Chem. **89**, 3642 (1985).
[32]I. B. Berlman, *Handbook of Fluorescence Spectra of Aromatic Molecules* (Academic, New York, 1971).
[33]A. Sur and P. M. Johnson, J. Chem. Phys. **84**, 1206 (1986).
[34]W. L. Hase and D. L. Bunker, program QCPE-234 (California Institute of Technology, Pasadena, CA).
[35]R. A. Marcus, W. L. Hase, and K. N. Swamy, J. Phys. Chem. **88**, 6717 (1984); R. A. Marcus, J. Chem. Phys. **85**, 5035 (1986).
[36]U. Schubert, E. Riedle, H. J. Neusser, and E. W. Schlag, J. Chem. Phys. **84**, 6182 (1986).
[37]R. E. Smalley, J. Phys. Chem. **86**, 3504 (1982).